RSC Advances

ROYAL SOCIETY OF CHEMISTRY

www.rsc.org/advances

Journal Name

ARTICLE

Clay catalysed rapid valorization of glycerol towards cyclic acetals and ketals

Radheshyam R. Pawar[a,b], Kalpeshgiri A. Gosai[a], Adarsh S. Bhatt[a], S. Kumaresan[a], Seung Mok Lee[*b] and Hari C. Bajaj[*a]

Biodiesel production usually results in a huge amount of glycerol, raising a critical need to transform it into high added value products. The present study highlights that solvent-free, conventional thermal activation, and non-conventional microwave/ultrasonic activation in the liquid phase are able to selectively transform glycerol into cyclic acetals and ketals using an optimised acid activated clay catalyst. Several parameters for the acid activation of bentonite clay were optimized under mild reaction conditions with a high concentration of clay (6%) and varying the acid concentration in the range of 6 to 15N. The alteration features of acid-activated clay were characterized by XRD, FT-IR, BET, and XRF analysis. The active sites of the catalyst were examined by volumetric titration and confirmed by pyridine adsorbed FT-IR and advanced NH_3-TPD analyses. The activation performed at relatively mild conditions, i.e.; 6N H_2SO_4 and 6% w/v clay, reproducibly resulted in an improved surface area (180 m^2 g^{-1}) and surface acidity (23 mg KOH g^{-1}), with superior quantitative Brönsted and Lewis acidic sites. Moreover, the eco-friendly process involving a catalyst, microwave, or ultra-sonication were successfully utilized to achieve commercially valuable hyacinth fragrance, in addition to furan-based fuel additive precursors exhibiting high conversion of glycerol and excellent selectivity within very less activation time (2 minute).

Received 00th January 20xx,
Accepted 00th January 20xx

DOI: 10.1039/x0xx00000x

www.rsc.org/

Introduction

The requirement of biofuels is continuously growing due to diminishing fossil fuel reserves.[1, 2] Biodiesel is one of the most promising and feasible alternatives among the unconventional sources of energy, however, biodiesel production results in a huge quantity of glycerol.[3] Global biodiesel production is estimated to yield ~4 billion gallons of glycerol by 2016.[4] Therefore, it is essential to develop viable methods to dispense or utilize the anticipated large quantity of glycerol, in order to add value to the biodiesel production chain.[5] These motives have triggered rigorous research in recent years with a view to finding applications for cheap and off grade glycerol by catalytic conversion processes including hydrogenolysis, oxidation, dehydration, polymerization, steam reforming, etherification, esterification, cyclization and acetalization.[6-10] In fact, glycerol derivatives such as acetal, ketal, ether, and ester find applications in the cosmetic, plastic, pharmaceutical, detergent, fuel additive and fine chemical industries.[11, 12] Particularly, acetalization of glycerol with furfural and its derivatives produces 1, 3-dioxalane and 1, 3-dioxane are used as fuel additives. These products enhance the viscosity and cold properties of biodiesel, in addition to improving the oxidation stability and flash point.[13] Traditionally, Brönsted acids such as HCl, H_3PO_4, and p-toluenesulfonic acid (PTSA) have been employed for the acetalization of glycerol in hazardous organic solvents to improve the conversion of glycerol.[6] However, such protocols poses a serious environmental concerns and thus improved catalytic processes are highly desirable wherein the use of expensive and toxic reagents, tedious work-up procedures, and the generation of large amounts of waste is avoided.[2] A variety of heterogeneous catalysts such as ion exchange resins,[14, 15] zeolites,[16] silica supported heteropoly acids,[17] acid functionalized carbon/silica,[18] supported activated carbon, and metal oxides, [19, 20] acidic ionic liquids,[21] Mg-Al-LDH as base catalyst[22] have been studied as catalyst for the acetalization of glycerol.

The modified clay minerals and their derivatives are a class of heterogeneous solid acid catalysts that has received considerable interest in diverse areas of organic synthesis due to their environmental compatibility, reusability, high selectivity, operational ease, non-corrosivenes, in addition their large availability in nature[23, 24]. One of the most common modifications of smectite clays is the treatment with mineral acid, usually HCl or H_2SO_4, resulting in the delamination of the clay structure.[25] A number of metal ions in the octahedral layer and impurities such as calcite are removed by leaching with an inorganic acid at elevated temperatures. In addition, the edges

[a] Central Salt and Marine Chemicals Research Institute (CSIR-CSMCRI), G.B. Marg, Bhavnagar-364002, Gujarat, India. Email:hcbajaj@csmcri.org and rrpawar84@gmail.com
[b] Department of Energy and Environment Convergence Technology, Catholic Kwandong University, 522 Naegok-dong, Gangneung, 210-701, Korea. Email:leesm@cku.ac.kr

of the platelets are opened, and as a result, the pore diameters and surface area of the clay is increased.[26] Acid activation promotes catalytic activity by increasing the number of Brönsted and Lewis acid sites.[25] The effect of acid concentration, time, and temperature during acid treatment on the surface acidity and physicochemical properties of the obtained clays have been well documented.[27] However, there has been little information on the systematic efforts to develop an optimized acid activation protocol under mild synthetic conditions with a high clay content to prepare clay catalyst in bulk. Numerous approaches have been employed to address the application of non-traditional activation methods such as microwave irradiation, sonochemistry, and solvent-free transformations for green organic syntheses.[28] The combined applications of heterogeneous catalysis with microwave or ultrasonic activation is a proficient and swift route to carry out chemical transformations, and becoming a widely accepted non-conventional protocol for organic synthesis.[29] The significant decrease in reaction time and the direct energy transformation via a solid catalyst is the unique combination of heterogeneous catalysis and microwave/ultrasonic irradiation that would also be more energy efficient than its conventionally-heated counterparts [30]. In continuation of our efforts towards the rapid valorisation of glycerol to value added acetals and ketals[31] herein we report the microwave- and ultrasonic-assisted catalytic protocol for the conversion of glycerol to value added acetals and ketals. Moreover, we have successfully utilized this sustainable and green protocol to achieve a commercially valuable hyacinth fragrance, in addition to furan-based fuel additive precursors in high glycerol conversion and selectivity.

Experimental

Materials

The clay mineral bentonite was collected from bentonite mines in the Banskantha district of Gujarat, India. Approximately 500 g raw bentonite lumps, after hot air drying, was grind in a mixer and passed through a 100 Mesh BSS sieve. The obtained sample was designated as BBnR (Banaskantha Bentonite Raw). The raw bentonite lumps were purified by sedimentation techniques, dried, grind, and passed through a 100 Mesh BSS sieve. This sample was designated as BBnU, (Banaskantha Bentonite Upgraded); (**S1** and **Table S1**). K10-Montmorillonite acid-activated clay, *p*-toluenesulphonic acid monohydrate (PTSA), Amberlyst 15 hydrogen form of acidic cation exchange, and fullers earth were obtained from Sigma Aldrich.

Chemicals

All the reagents, viz concentrated H_2SO_4 98%, glycerol, aldehydes, ketones, solvents, and other chemicals used for the experiments were of analytical reagent (A.R.) grade and were obtained from Merck, SD Fine, and Spectrochem. All the chemicals were used without further purification.

Catalyst synthesis

Acid activation experiments were performed using a clay concentration of 6% (w/v), optimized by varying the clay concentration in the range of 4 to 6 % under optimized activation conditions. Moreover a clay concentration beyond 6% (w/v) resulted in unsuitable mixing of the acid and clay due to swelling and the high viscous nature of the clay slurry. Hence, in order to achieve a homogenous mixture, a clay concentration of 6% (w/v) was used. The acid concentration was varied in the range of 6 to 15N. In detail experiments, precisely 60 g of purified clay was treated with a calculated amount of sulphuric acid, at 65°C for 10 hours. After completion of the reaction, the solid product was separated by centrifugation (Kubota 6500 centrifuge) and washed with deionized water. The washing cycle was repeated until the solid product was free from sulphate ions ($BaCl_2$ test), and the sample was subsequently dried at 110°C overnight. The solid activated product was ground by passing through a 100 Mesh BSS sieve. The obtained products were designated as N/BBnU/C, where N is the normality of sulphuric acid used for each experiment, and C is the percentage w/v clay concentration in the reaction mixture.

Physical measurements

The powder X-ray diffraction analysis was carried out with the Philips X pert MPD system in a 2θ range of 2–70°using Cu Kα (l= 1.54178Å) radiation. Nitrogen adsorption/desorption measurements for the evaluation of textural properties (surface area, total pore volume, and pore size distribution) were performed at 77 K using ASAP 2010, a surface area analyser, (Micrometrics USA). Prior to measurements, the samples were degassed at 423 K for 4 hours to remove any residual moisture. The BET specific surface areas were calculated from adsorption data in the relative pressure (P/P_0). Pore size and pore volume were calculated using the BJH method applied to the desorption leg of the isotherms. The FTIR spectroscopic measurements and diffuse reflectance FTIR (DRIFT) measurements were carried out using a Perkin Elmer GX spectrophotometer. Chemical analysis of the samples was carried out by X-ray fluorescence (XRF), using an S4 pioneer Bruker AXS XRF analyser. Bulk density measurement experiments were performed on the electro tab density tester (USP). ^{1}H and ^{13}C NMR spectra were recorded on a Bruker AX 200 MHz spectrometer at ambient temperature using TMS as an internal standard and $CDCl_3$ as a solvent. The reaction products were analysed using a gas chromatograph (Varian, GC–450), equipped with a Factor 4 capillary column (30 m long and 0.32 mm internal diameter) employed with a flame ionization detector. The oven temperature varied from 80 to 240°C, programmed at the ramp rate of 10°C min^{-1}. The GC oven was programmed in the temperature range of 40–200°C with helium as a carrier gas and the MS was programmed in EI mode with a 70 eV ion source. The calibration of the GC peak areas was carried out by taking solutions of known compositions with n-hexadecane as an internal standard. Product identification was performed using a gas

chromatograph mass spectrometer (Shimadzu GCMS-QP-2010, Japan) equipped with a RTX-5 fused silica capillary column.

Acidity measurements

pH and Titratable acidity

Acidity of the acid-activated clay was measured with pH measurement (Toshniwal pH meter at 30°C) by suspending 2.5 g clay in 25 ml distilled water (Table 1). Moreover, the acid activated clay has an acidity resulting from adsorbed sulphuric acid and aluminium sulphate. This acidity is determined by the so-called "boil-out" titration method. The acidity expressed in milligrams of KOH per gram of sample and is usually termed as "acidity". For preparing the effective catalysts, all acid activation conditions (i.e. effect of clay concentration, acid concentration, effect of activation temperature and time etc.) were optimized on the basis of "titratable acidity"(**S2.1**).

Ammonia TPD and pyridine FT-IR study

NH_3-temperature programmed desorption experiments were performed by using Auto-Chem 2910 instrument of Micromeritics. Exactly 200 mg of the catalyst was placed in a quartz tube and degassed at 423 K under the flow of helium. Then the ammonia gas was passed through the catalyst surface for 30 min and subsequently flushed with helium to remove the physisorbed gases. Then, the chemisorbed amount of NH_3 was determined in flowing helium gas with a flow rate of 20 mL min^{-1} from 323 to 873 K at a heating rate of 10 K min^{-1}.

Pyridine, a weak base is adsorbed on the clay surface through acid-base interactions. Pyridine is adsorbed on the Bronsted acid sites generated by the exchange of interlamellar cations with protons and $A1^{3+}$ present in octahedral sheet. For the FTIR analysis of adsorbed pyridine, samples were oven dried at 373 K for 3 h. The oven dried sample (~0.2 g), in a sample cup, was exposed to pyridine vapours in vacuum desiccators with 25 ml of dry pyridine. The sample cup was then kept in vacuum for 4 h, subsequently; the samples were evacuated for 30 min at room temperature to desorb physisorbed pyridine and FTIR spectrum was recorded in the spectral range of 1200–1900 cm^{-1} using a KBr disc.

Acetalization of glycerol

The catalytic performance of the synthesized catalyst was investigated for the acetalization of glycerol with aldehydes and ketones. In order to optimize the reaction conditions, the reaction of glycerol with cyclohexanone, which yields two isomeric products namely, 1, 3-dioxalane and 1, 3-dioxane, was studied as a model reaction. Typically, 1.0 g cyclohexanone and 0.93-2.79 g glycerol (varied reactant ratio) were fed to the reaction vessel along with 50 mg pre-activated catalyst (5% w/w to cyclohexanone) for each catalytic run. The reaction mixture was heated to the desired reaction temperature (27–60°C) for 0.5–19 hours. All experiments were carried out under vigorous stirring (700 rpm) to achieve a homogeneous mixture of glycerol and cyclohexanone. On completion of the reaction, catalyst was separated from the reaction mixture by centrifugation and then assignment of the products was confirmed by GC-MS and also by ^{1}H and ^{13}C NMR recorded in $CDCl_3$ at 200 MHz (**S4**).

The reaction performances were studied with respect to the conversion of aldehydes or ketones. The conversion and selectivity of the desired components were analysed by gas chromatography analysis (GC) with n-hexadecane used as an internal standard (IS). The calibration of the GC peak areas was carried out by taking standard solutions of known compositions with n-hexadecane as an internal standard. The conversion and selectivity were calculated as per the formulas (i) and (ii), respectively. (**S3**).

$$\%\ \text{Conversion}_{(\text{substrate})} = \frac{\{C_i - C_f\}_{(\text{substrate})}}{\{C_i\}_{\text{substrate}}} \times 100 \qquad \text{i}$$

$$\%\ \text{Selectivity}_{(\text{product})} = \frac{\{C_f\}_{(\text{product})}}{\{C_i - C_f\}_{(\text{substrate})}} \times 100 \qquad \text{ii}$$

where C_i and C_f are the initial and final concentrations of the respective species in the reaction mixture.

Acetalization of glycerol by Non-conventional heating

The microwave assisted synthetic manipulations were conducted using SINEO M-II microwave in a 25 ml RB flask synthesis assembly with variable MW frequency and temperature provision. The ultrasonic radiation assisted synthetic manipulations were conducted on Hielscher ultrasonic processor UP400S (Synthesis assembly with sonotrode H_3, variable frequency and adjustable pulse). Each set of reactions is treated under controlled sonication parameters by keeping 100 % amplitude and continuous probing. The typical acetalization reactions were carried out with a neat mixture of glycerol and aldehyde or ketones in presence of 50 mg catalyst and without solvent for pre-set time as required to complete the reaction. The conversion and selectivity were calculated as per the formulas (i) and (ii), respectively.

Results and Discussion

In the variation study of acid activation experimental conditions, It was observed that under mild acid activation conditions i.e., 6 to 8N, surface acidity was found to be in the range of 23 to 25 mg KOH g^{-1} whereas, in case of higher concentration (12 N and 15 N) a sudden decrease in surface acidity occurred 14 and 12 mg KOH g^{-1} respectively. Moreover, the % weight loss was found to be higher at harsh acid activation conditions (12 N and 15 N). Further alteration features of acid-activated clay were characterized by various physiochemical techniques (Table 1).

Table 1. Effect of acid activation conditions on the properties of bentonite clay, with an activation temperature 65°C, a reaction time of 10 hours, and a batch size of 60 g for each experiment.

Properties	Samples					
	BBnR	BBnU	6/BBnU/6	8/BBnU/6	12/BBnU/6	15/BBnU/6
Acid conc (N)	---	---	6	8	12	15
Acid:clay[1]	---	---	1	1.33	2	2.50
SA[2] (m^2/g)	87	74	180	209	302	308
APD[3] (nm)	5.1	5.2	5.2	5.5	6.5	6.2
Vt[4] (cc/g)	0.11	0.11	0.23	0.29	0.5	0.48
pH[5]	7.53	7.16	2.70	2.56	2.81	3.06
Acidity[6]	---	---	23	25	14	12
% Wt. Loss	---	---	20	24	38	50

[1]Normality of acid/% concentration of clay in suspension (w/v); [2]BET surface area (m^2/g); [3]Average pore diameter (nm); [4]Total pore volume (cc/g); [5]pH of the clay suspension (2.5 g of clay in 25 ml distilled water) measured via a toshniwal pH meter with 1% w/v clay at 30ºC. [6]Surface acidity mg KOH g^{-1} of the clay

XRF analysis for chemical composition

The XRF analysis was carried out to determine the chemical compositions of the clay and the subsequent chemical changes that occurred due to acid treatment. Table 2 shows the results of the chemical analysis of the purified and acid-activated bentonite samples. The BBnU clay contained SiO_2, Al_2O_3, and Fe_2O_3 in major quantities, whereas other oxides such as MgO, CaO, Na_2O, K_2O, and TiO_2 were present in trace amounts. During the acid treatment, it was observed that the composition of the parent clay changed considerably. As the strength of the acid increased, the amount of Fe_2O_3, Al_2O_3, MgO, CaO, K_2O and Na_2O in the acid-treated material decreased progressively.[32]

Table 2. Effect of acid activation conditions on chemical composition of activated bentonite clay.

% wt. oxide	BBnU	6/BBnU/6	8/BBnU/6	12/BBnU/6	15/BBnU/6
Na_2O	0.75	0.07	0.04	----	----
MgO	1.63	1.02	0.87	0.38	0.52
Al_2O_3	17.2	16.98	16.01	11.15	11.54
SiO_2	49.5	50.46	55.32	63.03	71.01
K_2O	0.84	0.69	0.53	0.26	0.15
CaO	0.60	0.07	0.06	0.03	0.06
TiO_2	3.07	3.10	3.22	3.58	1.28
Fe_2O_3	9.78	10.0	6.82	3.47	1.07
LOI	16.6	17.85	17.13	18.11	14.77
Total	**100**	**100**	**100**	**100**	**100**

X-ray diffraction studies

Powder X-ray diffraction (XRD) is one of the primary techniques used for tracking changes in the layer spacing of clay minerals. The strong basal reflection around 2θ = 5.97° is a common characteristic of calcium bentonite.[33] Powder X-ray diffraction patterns of bentonite samples from Banaskantha, before and after up gradation (BBnR and BBnU), were compared (Fig. 1 A and Fig 1 B). In beneficiated samples, the removal of the non-clay matter is reflected in the XRD patterns by the decrease in the intensities of the characteristic peaks of quartz after up gradation. The structural changes that occurred in the clay material due to acid treatment were also studied using X-ray diffraction (Fig. 1.). Generally, after acid activation, the '001' reflection appeared broad and weak due to the partial destruction of the layered structure of the smectite. The reduction in intensity and increase in width of the '001' peak indicates that the crystallinity of the 'BBnU' was considerably affected by acid activation. If the activation is conducted under harsh acidic conditions, the '001' reflection would completely disappear, with the process favouring the production of the amorphous phase by decomposing of the clay structure. The acid treatment used for the synthesis of 6/BBnU/6 and its activation process did not damage the inherent layered structure of bentonite. Here this can assume that the structure has been partially destroyed. The balance between acid treatment and structural preservation hold the key for the establishment of optimal catalytic parameters (Fig. 1.). An increase in acid concentration to 8N (H_2SO_4) showed slight reduction in the peak intensity of the '001' plane, indicating the stacking disorder of the layers. Further increments in acid concentration of 12-15 N H_2SO_4 resulted in even broader '001' reflection peaks than that of activated samples synthesized under mild conditions. However the '020' and '060'peaks of 'BBnU' remained unchanged by 12-15 N H_2SO_4 acid activation.

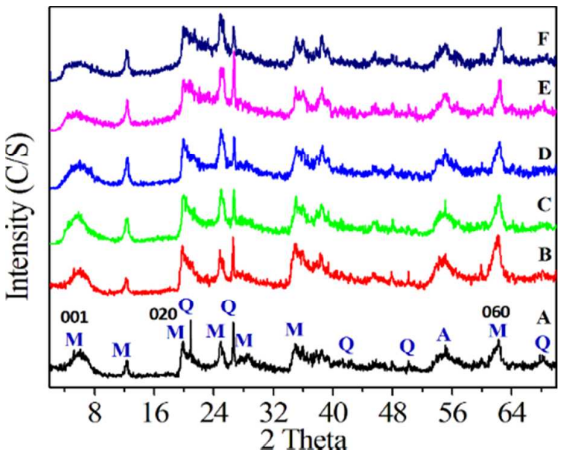

Fig. 1. Powder X-ray diffraction patterns of [A]: BBnR, [B]: BBnU, [C]: 6/BBnU/6, [D]: 8/BBnU/6, [E]: 12/BBnU/6, [F]: 15/BBnU/6. Where, M: Montmorillonite, Q: Quartz, A: Anatase.

Infrared spectroscopic studies

The spectra of original, purified bentonite and the samples treated with 6-15 N H_2SO_4 acid concentrations are shown in Fig. S1. The spectrum of the original clay exhibits absorption bands at 3441 and 1636 cm^{-1} assigned to the stretching and bending vibrations of the OH groups of the water adsorbed on the clay surface, and a band at 3617 cm^{-1} representing the stretching vibration of the OH groups coordinated to octahedral Al^{3+} cations. The Si–O bands are strongly evident in the silicate structure of the original clay, and can be easily recognized in the infrared spectrum as very strong absorption bands in the 1100–1000 cm^{-1} region. The most intensive band

at 1039 cm^{-1} is attributed to Si–O in plane stretching and the band at 1127 cm^{-1} is due to Si–O out of plane stretching vibration. The bands at 537 and 474 cm^{-1} correspond to Si–O–Al (octahedral) and Si–O–Si bending vibrations, respectively. The FTIR spectrum of raw clay depicts a band at 794 cm^{-1} attributed to cristobalite phase. The treatment of bentonite with 12 and 15 N H_2SO_4 acid resulted in the formation of amorphous silica, which complements the data obtained from PXRD. The intensity of the absorption bands at 907 cm^{-1} decrease due to leaching and partial depletion of Al, Mg, and Fe from the clay structure, in accordance with the changes in chemical composition. The intensity of the bands at 3441 and 1636 cm^{-1} for water of hydration and the hydroxyl stretching band at 3617 cm^{-1} also show a significant decrease after acid activation. However, the persistence of a weak band at 1039 cm^{-1} indicates that the layered structure of the original clay is not fully destroyed, which is in agreement with the XRD results. The progressive widening of the 1039 cm^{-1} bands, together with the increase in intensity of the 795 cm^{-1} band (tridymite), indicates the formation of amorphous silica.[34] In conclusion, an IR spectrum of activated clays indicates that acid leaching affects both the octahedral and the tetrahedral sheets.[35, 36]

Textural properties

The N_2 adsorption and desorption isotherms of the raw, purified and acid-activated clay samples are presented in Fig. S2. The isotherms of these samples are of type IV according to the IUPAC classification.[37] The hysteresis loop indicated the presence of the slit pores with the capillary condensation of liquid nitrogen on its mesopores.[38, 39] The most important textural change in acid-activated clays was an increase in the specific surface area (SA) and the pore volume (PV) due to splitting of particles within the leached octahedral sheets. The extent of these changes depended on the activation conditions such as acid strength, temperature, and length of the treatment. The textural properties of the samples before and after acid treatment are given along with upgraded bentonite in Table 1. An approximate 2.4 times increase in SA and a 2 time increase in PV was observed after treatment with 6 N H_2SO_4 acid. When the acid concentration was increased to 15 N, SA and PV of the treated sample increased by 3.5 and 4.5 times, respectively, indicating the formation of amorphous silica with high SA and PV. The BJH pore diameter and average pore diameter of all the acid-activated samples were almost similar, indicating the narrow pore size distribution. Similar trends in the textural change results have been observed in previous reports.[27, 32]

Acidity measurements

The total acidity of activated clays is higher than that of the pristine bentonite sample because of the replacement of exchangeable cations with protons. The acidic properties of bentonite also originated from the presence of (1) terminal hydroxyl groups, (2) bridging oxygen, and (3) the dissociation of interlayer water molecules coordinated to the exchangeable cations.[27] The total acidity of various clays samples by pH measurements on aqueous clay suspensions (Table 1) shows that acidity increases from 'BBnU' (pH 7.16) to 6BBnU6 (pH 2.70) after which it shows a decreasing trend for the acid treated samples under harsh conditions

The NH_3 TPD patterns for acid activated samples and desorption peak areas are shown in Fig. 2 and Table S2. The relative position of the peak maxima (**Fig 2)** is an evidence of the magnitude of the ammonia desorption activation energy, which indicates the relative strength of the acidic sites.[2] It can be noted from NH_3-TPD study that the harshness in acid activation conditions decreases the acidic strength as well as its concentration. The total peak area due to ammonia in ammonia TPD plot (concentration for amount of acidic sites) was found to be ~3.15, 2.57, 1.44 and 1.33% for the 6/BBnU/6, 8/BBnU/6, 12/BBnU/6 and 15/BBnU/6 respectively (Fig.2 and Table S2**).**

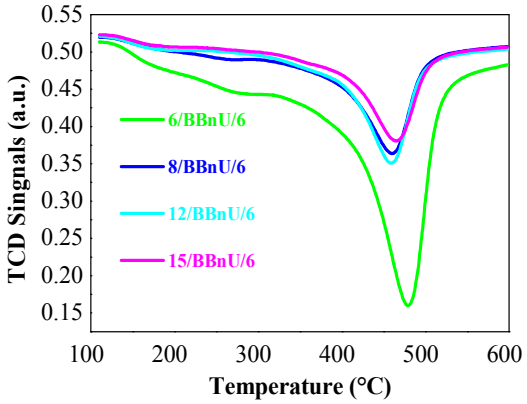

Fig.2. NH_3 TPD profiles of the acid-activated bentonite samples

The activated sample, 6/BBnU/6 shows the highest acidity among all other samples considered for this study which indicates presence of maximum number of acidic sites on it. The result corroborates well with those obtained from volumetric titration experiments. Moreover, the observed difference between acidic properties of 6/BBnU/6 and 8/BBnU/6 indicated by KOH titration and TPD experiments is worth mentioning. Since the KOH treatment of clay samples involve 'boil-out' titration which employs rather drastic conditions than the TPD experiment. It is inferred that during KOH titration 8/BBnU/6 sample exfoliate and leach metal ions from octahedral sites are responsible for observed acidity. However, TPD being more sophisticated technique render acidic properties more precisely. This observation and inference also helped us to screen and chose the superior catalyst among all, i.e., 6/BBnU/6.

Fig. S3 shows the IR spectra recorded after pyridine adsorption on acid-activated clay samples and unmodified BBnU. The IR spectra of 6/BBnU/6 exhibit prominent vibration bands at 1638, 1543, 1491, and 1443 cm^{-1}. The bands at 1545-48 cm^{-1} were assigned to Brönsted pyridine sites; however, those at

1445-47 and 1600 cm^{-1} are due to hydrogen bonding between the pyridine nitrogen and -OH groups of the clay minerals. A strong band at 1492 cm^{-1} indicates the combined presence of all acid sites (Lewis py + Brönsted py + Hydrogen bonding)[40]. It is noticeable from the figure S3 that activated 6/BBnU/6 exhibits a high intensity Brønsted and Lewis acid sites peaks compared to other acid activated samples and pristine BBnU. These data also support earlier conclusion that harshness in acid activation conditions decreases the acidic strength.

Catalyst screening

Fig.3. presents the effect of different activation conditions on the performance of materials in terms of surface acidity, surface area, and the final yield of product. Among all the synthesized materials, 6/BBnU/6 and 8/BBnU/6 were found to be superior, and specifically considering the mild synthetic protocol, and yield of product. Pushpaletha and co-workers [42] reported that the iron and aluminium content in acid-activated clay plays a crucial role in the catalytic activity. The Al_2O_3 and Fe_2O_3 content were highest in 6/BBnU/6 after acid activation (Table 2), which corroborates with the observed highest acidity. The higher Al_2O_3 and Fe_2O_3 content results in the expulsion and relocation of the octahedral cations, Al^{3+} and Fe^{3+}, between the interlayer space under optimum acid activation conditions. Considering the above merits, the 6/BBnU/6 sample was selected for further catalytic applications.

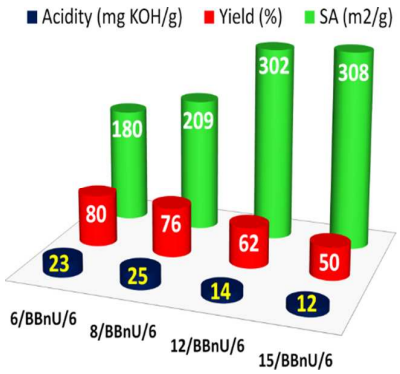

Fig. 3. Relative effects of sample preparation protocols on the product yield, acidity, and surface area.

Acetalization of glycerol with cyclohexanone

In order to evaluate the catalytic activity of optimized activated clay (6/BBnU/6), the reaction of glycerol with cyclohexanone yielding isomeric products 1,3-dioxalane (1,4-dioxaspiro [4.5]decan-2-ylmethanol) and 1,3-dioxane (1,5-dioxaspiro[5.5]undecan-3-ol) was studied as a model reaction (**Scheme 1**). The reaction outcomes were studied with respect to temperatures, time, and molar ratios of the reactant. The analysis of the raw reaction products were performed by gas chromatography (GC). Typically chromatograph exhibited two product peaks, first broad and high intesity peak with retention time 8.67 min for 1,4-dioxaspiro [4.5]decan-2-ylmethanol (Five membered 1,3-dioxalane) and second small and low intesity peak with retention time 9.01 min for (1,5-dioxaspiro[5.5]undecan-3-ol) (six membered 1,3-dioxalane) confirmed by and gas chromatograph with mass spectrometry (GC-MS) (**Fig. S5),** ^{1}H and ^{13}C NMR **(S3).** With regards to the selectivity of the catalytic reactions, the cyclohexanone was found more reactive cyclic substrate for glycerol acetalization. The sectivity of five membered 1,3-dioxalane (i.e. 1, 4-dioxaspiro [4, 5] decane-2-methanol) was found in the range of 94-100% [6, 43]. Moreover, the acetalization reaction between glycerol and cyclohexanone can be kinetically or thermodynamically controlled.[44] During the kinetically-controlled reaction, the formation of five-membered cyclic ketals proceeds at a higher rate than that of the six-membered cyclic ketals.[44]

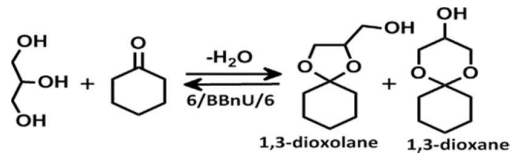

Scheme 1: Glycerol acetalization with cyclohexanone.

Reaction at room temperature (26-28°C)

Initially the catalytic experiments were carried out at room temperature under solvent-free conditions with 1:1, 1:2, and 1:3 molar ratios of cyclohexanone to glycerol for a reaction time of 1-19 hours. The results obtained in terms of cyclohexanone conversion and the selectivity of five-membered cyclic 1,3-dioxalane and six-membered cyclic 1,3-dioxane are summarised in Table 3.

Table 3: Acetalization of glycerol with cyclohexanone at RT (26-28°C) and mild temperature conditions.

Time (hr)	Cyclohexanone: Glycerol moles								
	1:1			1:2			1:3		
	[a]I	[b]II	[c]III	[a]I	[b]II	[c]III	[a]I	[b]II	[c]III
3	45	99	01	65	87	13	**78**	**89**	**11**
8	67	90	10	**81**	**89**	**11**	83	90	10
19	80	92	08	87	92	08	90	92	08
0.5[#]	--	--	--	86	98	02	--	--	--
1[*]	**70**	**96**	**04**	**92**	**98**	**02**	93	98	02

[a]Conversion of cyclohexanone,[b] % Selectivity of 5-membered cyclic ketal, [c] % Selectivity of 6-membered cyclic ketal. [*]Reaction conditions: catalyst amount = 5% wt (w.r.t. cyclohexanone), reaction temperature: 60ºC and reaction time = 1 hr. [#] Reaction conditions: catalyst amount = 5% wt (w.r.t. cyclohexanone), reaction temperature: 60ºC and reaction time = 30 min.

When the acetalization reaction of glycerol and cyclohexanone was carried out with an equimolar ratio for a period of 3, 8, and 19 hours, the conversion of cyclohexanone was 45, 67, and 80%, respectively. These conversion values improved to 65, 81, and 87%, respectively, when the molar ratio of cyclohexanone to glycerol was increased to 1:2, the use of excess glycerol than equimolar results in high conversion. The reason for these high conversions is not generic and may be specific to certain reactions. However, one reason that may contribute to higher conversion is the hydrogen bonding present in the glycerol molecule. It is

worthy to mention here that the glycerol is increasingly being used as a greener solvent for organic transformations for various reasons such as its polarity, structure and solvent solubility properties resulting in higher yields[12, 45]. A further increase in the molar ratio to 1:3 showed 78, 83, and 90% conversion, respectively, at identical reaction times. Since the higher molar ratio of cyclohexanone to glycerol (1:3) did not show significant improvement in the conversion or selectivity of products after 8 and 19 hours, hense 1:2 molar ratio was chosen as the optimum stoichiometry for the acetalization reactions with 5% catalyst loading at room temperature for 8 hours. The reaction time was further optimized by studying the acetalization of cyclohexanone with glycerol with a molar ratio of 1:2 for different time intervals. The conversion reaction gradually increased with time and 87% with 92% selectivity of the five-membered cyclic ketal after 19 hours was found (Fig. 4 [A]).

Effect of conventional heating

The influence of temperature on the 6/BBnU/6 catalyzed reaction was studied by increasing the reaction temperature from 27 to 100°C, while the reactant ratio was kept at 1:2 for each set of reactions. As expected, an increase in temperature increased the conversion and selectivity of the products (Fig. 4[B]). When the temperature was kept at 60°C, and the reaction was allowed to progress for 1 hour, 90-94% conversion and 99% selectivity for five-membered ketals was observed. Above 60°C no significant improvement in conversion or selectivity was noted, thus, 60°C was chosen as the optimum temperature for further studies.

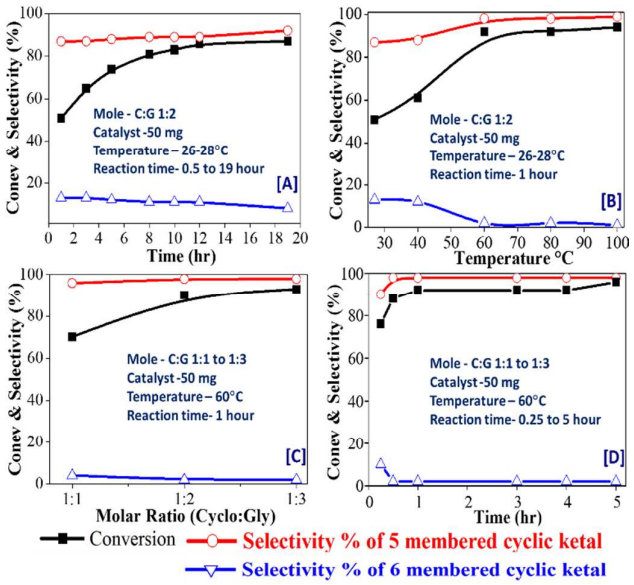

Fig.4. Influence of reaction parameters on glycerol cyclohexanone acetalization over the 6/BBnU/6catalyst, [A] Reaction time, [B] Reaction temperature, [C] Reactant molar ratio, [D] Reaction time at a temperature of 60ºC.

Effect of molar ratio (60°C)

The effect of the cyclohexanone to glycerol molar ratio on the cyclohexanone conversion was studied at room temperature and 60°C. The obtained results suggest that a 1:2 mole ratio of reactants yields the maximum cyclohexanone conversion. These results also indicate that the experiment performed at 60°C for 1 hour yields better results than the reaction carried out at room temperature for 19 hours (Table 3; entry 1*). The dependence of cyclohexanone conversion on the reaction time, with the optimum molar ratio and temperature conditions, was studied (Fig. 4[C]). At the optimized temperature (60°C), the acetalization reaction progressed faster than at room temperature.

Effect of reaction time (60°C)

The experiment performed at the optimum temperature conditions for 30 minutes gave 86% conversion of cyclohexanone. These results are better than those obtained at room temperature for the reaction carried out for 19 hours (Table 3; entry 0.5#). The reaction under the optimized conditions was monitored for 5 hours, and the conversion and selectivity was maximum within 2 hours (Fig. 4.[D]). However, the optimum time was considered to be 1 hour, as the results achieved in a 1 hour reaction time were comparable with the longer reaction times.

Effect of catalyst loading (60°C)

The catalytic experiments were conducted by varying the amount of catalyst from 1 to 7 wt % and keeping the other experimental conditions identical to those optimized. Interestingly, the optimised catalyst exhibited better cyclohexanone conversion at 4 to 7wt% cataltst. With the increase in the catalyst amount, the glycerol conversion increased being attributed to the availability of a higher number of acidic sites. At 5% wt of the catalyst, the glycerol conversion was 90% and the selectivity between 1,3-dioxane and 1,3-dioxolane was 98:2. However, with a further increase in the amount of catalyst, there was no considerable change in the cyclohexanone conversion or selectivity of the products.

The typical acetalization reaction ran under optimized conditions showed 90-92% conversion and 98 and 2% selectivity for five-membered 1,3-dioxalane and six-membered 1,3-dioxane, respectively.

Considering the commercial importance of the acetalization reactions, the model reaction was scaled up to 100 ml, resulting in 88% conversion and consistent selectivity. For the sake of comparison, the model reaction was performed under identical optimized conditions in the absence of the catalyst, which showed only 10-15% conversion of cyclohexanone. This result indicates the role of the catalyst in accelerating the rate of the reaction (Table 4; entry 1).

Confirmation of catalyst screening

The clay samples were activated by 6 N to 15 N sulphuric acids at a 6% clay concentration. The acid-activated clay samples were screened as a catalyst for acetalization of cyclohexanone with glycerol under optimum conditions. Among the various

catalysts, the highest cyclohexanone conversion (90-92%) along with 98% selectivity for the five-membered 1, 3-dioxalane was obtained from the clay samples activated with 8 N and 6 N acid concentration, which possess higher surface acidity (25 and 23 mg KOH g^{-1} of clay). The conversion decreased with increasing acid concentrations (12 N and 15 N) used for activation **(Table S3).** These results clearly demonstrate that catalytic activity increased with an increase in the surface acidity of the acid-activated samples. As clay catalysts consist of several metal oxides which contribute towards the acidity of material. It is very hard to ascertain exact details about the active sites of these catalysts. Hence the TON and TOF were not calculated. However, the comparison with respect to surface area in incorporated (Table S3) for comprehension.

The unmodified sample 'BBnU' was also screened for acetalization of cyclohexanone under optimum conditions, which gave no acetalization products, suggesting that the acetalization reaction is promoted due to the available acidic sites on acid-modified bentonite (Table 4; entry 2).

Comparison with commercial catalysts

For the sake of comparison, the catalytic activity of some commercially available solid acid catalysts was also evaluated under the optimised reaction parameters. Thus, the commercially available clay catalyst K10 Montmorillonite showed 88% conversion and 96% selectivity for the cyclic five-membered ketal. Fuller's earth clay catalyst showed 86% cyclohexanone conversion with 94% selectivity for the five-membered cyclic ketals. Similar experiments in the presence of Amberlyst-15 showed 63% conversion and 87% selectivity for the five-membered cyclic acetals. The homogeneous PTSA catalyst showed 94% cyclohexanone conversion and 99% selectivity for the five-membered cyclic acetals (Table 4; entry 3-6). The catalytic activity of the optimised 6/BBnU/6 catalyst was compared with some earlier reports (Table 4; entry 7-8)[6].

Table 4: Glycerol acetalization with selective aldehydes and ketones under various experimental conditions, relative data from previous reports

Entry	Catalyst	Temp (ºC)	Time (h)	Mole Cyc:Gly	Conversion (%)	Selectivity (%)		Ref.
						5-M (%)[a]	6-M(%)[b]	
Cyclohexanone glycerol acetalization data for finest catalyst screening								
1	Catalyst free	60	01	1:2	15	84	16	--
2	BBnU	60	01	1:2	Trace	Trace	Trace	--
Cyclohexanone glycerol acetalization data comparison with commercial catalyst								
3	K10 MMT	60	01	1:2	84	96	04	--
4	Fullers Earth	60	01	1:2	86	94	06	--
5	Amb-15	60	01	1:2	63	87	13	--
6	PTSA	60	01	1:2	94	99	01	--
Cyclohexanone glycerol acetalization from literature reports								
7	$[Cp^*IrCl_2]_2$	40	01	1:3	59	94	06	6
8	$[Cp^*IrCl_2]_2$	40	02	1:3	76	97	03	6
Benzaldehyde glycerol acetalization data experimental								
9	Catalyst free	60	01	1:2	37	64	36	--
10	6/BBnU/6	RT	15	1:2	81	56	44	--
11	6/BBnU/6	60	01	1:2	84	60	40	--
12	6/BBnU/6	60	01	1:1	64	60	40	--
Benzaldehyde glycerol acetalization from literature reports								
13	MOO_3/SiO_2	100	16	1:1.1	70	30	70	20
14	$[Cp^*IrCl_2]_2$	40	01	1:3	55	79	21	6
15	$[Cp^*IrCl_2]_2$	40	02	1:3	67	78	22	6
16	$RHASO_3H$	120	08	1:2	78	67	33	46
Phenyl acetaldehyde glycerol acetalization data experimental								
17	Catalyst free	60	01	1:2	--	--	--	--
18	6/BBnU/6	RT	15	1:2	62	08	92	--
19	6/BBnU/6	60	01	1:2	68	09	91	--
20	6/BBnU/6	60	01	1:1	58	10	90	--
Phenyl acetaldehyde glycerol acetalization from literature reports								
21	MoO_3/SiO_2	100	08	1:1.1	56	09	91	20
22	Zeo-USY-2	150	02	1:2	95	64	31	47
Furan-2-carbaldehyde glycerol acetalization data experimental								
23	Catalyst free	60	01	1:2	--	--	--	--
24	6/BBnU/6	RT	15	1:2	72	57	43	--
25	6/BBnU/6	60	01	1:2	69	54	46	--

[a] and [b] represent five- and six-membered cyclic acetal/ketal products, respectively

Journal Name

ARTICLE

Catalyst stability tests

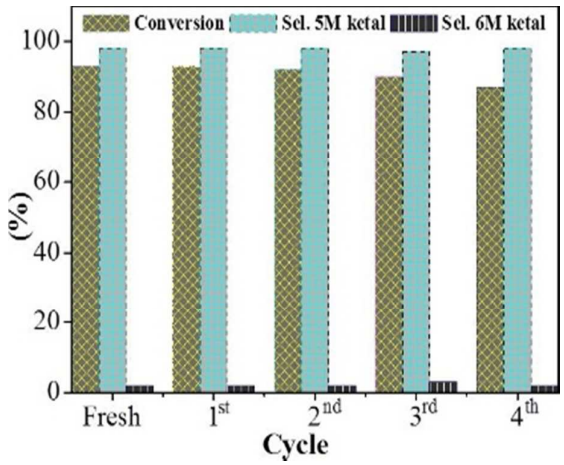

Fig.5. Catalyst recycling test under the optimized reaction conditions.

In order to study the stability and reusability of the catalyst 6/BBnU/6, the catalyst was successfully reused four times. A slight decrease in conversion after 4th run was observed. Each operating cycle was carried out at a temperature of 60 °C and a cyclohexanone to glycerol molar ratio of 1:2 for one h reaction time. The catalyst used was recovered by centrifugation, washed with water and methanol, and finally dried at 110°C for 2 hours. Fig.5. shows the results of cyclohexanone conversion and the selectivity of the five- and six-membered cyclic ketals for each reaction cycle. It is observed that there was no significant deactivation of the catalyst under the optimized conditions after fourth cycle**.**

Glycerol Acetalization with Benzaldehyde

The catalytic activity of 6/BBnU/6 was tested in the acetalization reaction between Benz aldehyde and glycerol, which yielded two isomeric products, a five-membered cyclic 1, 3-dioxalane acetal [(2-phenyl-1, 3-dioxolan-4-yl) methanol] and a six- membered cyclic 1, 3-dioxane [2-phenyl-1, 3-dioxan-5-ol] as depicted in Scheme 2.

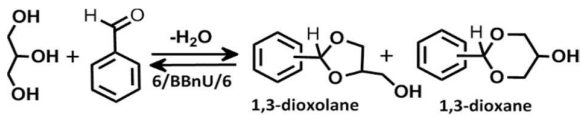

Scheme 2: Glycerol acetalization with benzaldehyde.

The five- and six-membered products were characterized by GC chromatograph (Fig. S6) with GC-MS and the crude reaction products were re-confirmed by ^{1}H and ^{13}C NMR (**S4).** The performance of the reaction was monitored with respect to temperature, time, and glycerol molar ratio. The obtained results of Benzaldehyde conversion and selectivity of the products are summarized in Table 4; entry 9-12. The experiment was performed at room temperature with reaction time of 15 hours, and the other parameters were kept identical, resulting in 81% conversion of benzaldehyde with 56% selectivity of five-membered cyclic acetals. While experiment performed at 60 °C and 1h reaction time resulting in 84 % conversion of Benzaldehyde with 60% selectivity of five-membered cyclic acetals. Interestingly shows that by increasing reaction temperature the reaction time diminishes considerably. The reaction of Benzaldehyde with glycerol in the absence of catalyst, under optimised reaction conditions resulted 37% conversion, which clearly specifies the role of the catalyst in accelerating the reaction. The catalytic activity of the optimised 6/BBnU/6 for benzaldehyde acetalization reaction was compared with earlier reports.[6, 20, 46] (Table 4; entry 9-12).

Hyacinth fragrance and fuel additives

The phenyl acetaldehyde glycerol acetals are flavouring materials with a hyacinth fragrance, and are synthesised by reacting the phenyl acetaldehyde with glycerol, yielding five-membered cyclic acetal [(2-benzyl-4-hydroxymethyl-1, 3-dioxolane)] and six-membered cyclic acetal [2-benzyl-5-hydroxy-1, 3-dioxane], along with the two geometrical isomers [47] **(Scheme 3). (Fig. S7)**

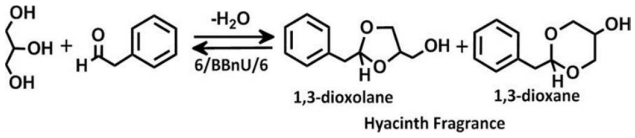

Scheme 3: Glycerol valorised as commercially important furan-based fuel additive precursors.

The acetalization of phenyl acetaldehyde with glycerol was carried out in the presence of the 6/BBnU/6 catalyst. The performance of the reaction was monitored with respect to temperature, time and glycerol molar ratio. The obtained results for phenyl acetaldehyde conversion and selectivity of the products are summarized in Table 4; entry 17-20. In the absence of a catalyst, the reaction of phenyl acetaldehyde with glycerol under optimised reaction conditions results in no conversion of phenyl acetaldehyde. The catalytic activity of the optimised 6/BBnU/6 catalyst for the hyacinth fragrance was

substantial as compared to earlier reports[47] (Table 4; entry 21-22). In another attempt to utilize our synthetic methodology to achieve commercially valuable products, we successfully synthesized the fuel additive precursors from furfural and glycerol, which yielded the five-membered cyclic acetal [(2-(furan-2-yl)-1, 3-dioxolan-4-yl) methanol] and the six-membered cyclic acetal [2-(furan-2-yl)-1, 3-dioxan 5-ol] **(Scheme 4), (Fig. S8) u**nder optimum conditions over the 6/BBnU/6 catalyst.

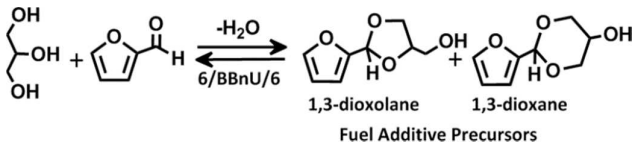

Scheme 4: Glycerol valorised as commercially important furan-based fuel additive precursors.

The performance of the reaction was monitored with respect to temperature, time, and glycerol molar ratio. The obtained results for furfural conversion and selectivity of the products are summarized in Table 4; entry 23-25. In the absence of a catalyst, the reaction of furan aldehyde with glycerol under optimised reaction conditions does not result in the formation of fuel additives.

Acetalization with other aldehydes/ketones

Table 5: Glycerol acetalization with other aldehydes/ketones, with an aldehyde/ketone glycerol molar ratio of 1:2, an IS of 200 µl, a reaction temperature of: 60ºC, a reaction time of 1 hour, and a catalyst of 5% wt aldehydes/ketone.

Entry	Substrate	Conversion (%)	Selectivity 5-M[a] (%)	Selectivity 6-M[b] (%)
1	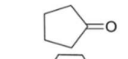	67	93	07
2	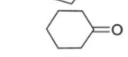	92	98	02
3	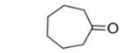	40	99	01
4	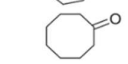	23	98	02
5	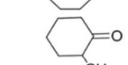	30	20	80
6	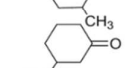	59	43	57
7	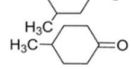	85	59	41
8	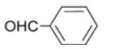	81	60	40
9	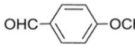	69	75	25
10	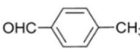	37	87	13
11	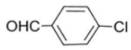	88	63	37
12	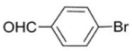	83	53	47
13	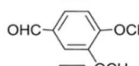	68	43	57
14	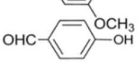	57	61	39

[a] and [b] represent five- and six-membered cyclic acetals/ketals products respectively.

The use of the optimised protocol was further extended for acetalization of several aldehydes and ketones. The high selectivity for five-membered ketals was achieved for cyclopentanone (93% selectivity; 67% conversion) and cycloheptanone (99% selectivity; 40% conversion), where the decrease in conversion may be attributed to the geometrical hindrance posed by five- and seven-membered ring conformations. A noticeable effect of steric factors in the conversion and selectivity was also observed for methyl cyclohexanones. Specifically, 2-methyl, 3-methyl, and 4-methyl cyclohexanone showed 30, 59, and 85% conversion with 20, 43, and 59% selectivity for five-membered ketals, respectively. The reversal of selectivity in the case of 2-methylcyclohexanone may be attributed to the steric repulsion between the methyl and hydroxyl groups residing in proximity to each other. The detailed results of conversion and selectivity of various aldehydes and ketones are summarised in **Table 5.** Different aldehydes showed a moderate selectivity, while ketones showed excellent selectivity. The electron donating or electron withdrawing substituent on the phenyl ring of benzaldehyde affects the conversion as well as the selectivity. An increase in selectivity (75%) of five-membered products was observed in the case of methoxy substituted benzaldehyde, with a slight decrease in the conversion (69%). In case of chloro, bromo, and other electron withdrawing substituents, the conversion of aldehydes and the selectivity of respective products remained unaffected.

Non-traditional pathways for glycerol Acetalization

Table 6: Alternative (non-traditional) pathways for glycerol acetalization with significant aldehydes and ketones.

Aldehydes/Ketone	Alternative energy inputs								
	Conventional (60 °C)			Microwave (60 °C)			Ultrasonic		
	[a]I	[b]II	[c]III	[a]I	[b]II	[c]III	[a]I	[b]II	[c]III
Time (minute)	**60**			**2**			**2**		
Cyclohexanone	92	98	02	92	98	02	89	97	03
Benzaldehyde	81	60	40	83	57	43	81	56	44
Ph-acetaldehyde	68	9	91	92	15	85	83	10	90
Furan aldehyde	69	54	46	78	48	52	77	58	42

[a] Conversion of aldehyde or ketone,[b] % Selectivity of 5-membered cyclic acetal and ketal, [c]% Selectivity of 6-membered cyclic acetal and ketal.

Furthermore, the optimized catalyst was tested in non-traditional microwave and ultra-sonication synthesis pathways, distinctly under solvent- free conditions. The influence of ultra-sonication time on cyclohexanone conversion and selectivity is depicted in **Fig. S4**. The obtained results suggest that a rapid two minute ultrasonic cavitation effect was enough for 89% conversion of cyclohexanone with 97% selectivity of five-membered cyclic ketals. Correspondingly, a 2-minute core heating under microwaves is sufficient for 92% conversion of cyclohexanone with 98% selectivity of five-membered cyclic ketals**.** The expected similar rapid conversion results were observed for hyacinth and furan-based fuel additives with the use of microwave and ultra-sonication synthesis pathways. The conventional reflux setup is relatively slow and inefficient to transfer the energy into a

reaction mixture, as it relies on convection currents and the thermal conductivity of the media (reaction vessel, reactants, and solvent phase, etc.), therefore the results obtained by conventional heating, owing to the longer reaction time, are slightly inferior when compared to the ultrasonic and microwave irradiation pathways (**Table 6**).

Conclusion

In summary, we developed a green heterogeneous process to synthesize industrially useful chemicals from the acetalization of glycerol. A solid acid catalysts from naturally abundant bentonite were prepared by simple acid activation under mild synthetic conditions. During the acid treatment, the parent clay composition was considerably changed. The specific surface area and pore volume of 6 N H_2SO_4-treated clay was found to increase by ~2.4 and ~2 times respectively. The synthesized catalyst has been efficiently employed for the valorisation of glycerol by means of an optimized mild and eco-friendly process. The catalytic chemical up gradation of glycerol was further shown to be more efficient and cost effective by using the non-conventional energy sources such as microwave irradiation and ultra-sonication. The development process could be efficiently applied to the solvent-free acetalization of several aldehydes and ketones with glycerol to produce corresponding acetals or ketals in high yields. Moreover, we successfully utilized this sustainable and green protocol to achieve commercially valuable hyacinth fragrance as well as furan based fuel additive precursors in good conversion and selectivity of the products.

Acknowledgements

The authors are grateful to the Council of Scientific and Industrial Research (CSIR) India for financial support under the Network project. RRP acknowledges CSIR, New Delhi for the fellowship. The authors also thank the Analytical Science Discipline of the Institute for instrumentation facility.

Notes and references

1. R. Luque, J. C. Lovett, B. Datta, J. Clancy, J. M. Campelo and A. A. Romero, *Energy & Environmental Science*, 2010, **3**, 1706.
2. B. Mallesham, P. Sudarsanam and B. M. Reddy, *Catalysis Science & Technology*, 2014, **4**, 803-813.
3. C. H. Zhou, J. N. Beltramini, Y. X. Fan and G. Q. Lu, *Chemical Society reviews*, 2008, **37**, 527-549.
4. M. Koberg and A. Gedanken, *Energy & Environmental Science*, 2012, **5**, 7460.
5. S. Bagheri, N. M. Julkapli and W. A. Yehye, *Renewable and Sustainable Energy Reviews*, 2015, **41**, 113-127.
6. C. Crotti, E. Farnetti and N. Guidolin, *Green Chemistry*, 2010, **12**, 2225.
7. A. Behr, J. Eilting, K. Irawadi, J. Leschinski and F. Lindner, *Green Chem.*, 2008, **10**, 13-30.
8. S. I. a. A. V. Avelino Corma, *Chem.Rev.*, 2007, **107**, 2411-2502.
9. P. Gallezot, *Chemical Society reviews*, 2012, **41**, 1538-1558.
10. M. J. Climent, A. Corma and S. Iborra, *Green Chemistry*, 2014, **16**, 516.
11. L. Moity, A. Benazzouz, V. Molinier, V. Nardello-Rataj, M. K. Elmkaddem, P. de Caro, S. Thiébaud-Roux, V. Gerbaud, P. Marion and J.-M. Aubry, *Green Chem.*, 2015, **17**, 1779-1792.
12. J. I. García, H. García-Marín and E. Pires, *Green Chemistry*, 2014, **16**, 1007.
13. B. L. Wegenhart, S. Liu, M. Thom, D. Stanley and M. M. Abu-Omar, *ACS Catalysis*, 2012, **2**, 2524-2530.
14. M. B. Güemez, J. Requies, I. Agirre, P. L. Arias, V. L. Barrio and J. F. Cambra, *Chemical Engineering Journal*, 2013, **228**, 300-307.
15. X. Hong, O. McGiveron, A. K. Kolah, A. Orjuela, L. Peereboom, C. T. Lira and D. J. Miller, *Chemical Engineering Journal*, 2013, **222**, 374-381.
16. M. Pagliaro, R. Ciriminna, H. Kimura, M. Rossi and C. Della Pina, *Angewandte Chemie*, 2007, **46**, 4434-4440.
17. A. Patel and N. Narkhede, *Energy & Fuels*, 2012, **26**, 6025-6032.
18. D. Nandan, P. Sreenivasulu, L. N. Sivakumar Konathala, M. Kumar and N. Viswanadham, *Microporous and Mesoporous Materials*, 2013, **179**, 182-190.
19. S. Zhang, Z. Zhao and Y. Ao, *Applied Catalysis A: General*, 2015, **496**, 32-39.
20. S. B. Umbarkar, T. V. Kotbagi, A. V. Biradar, R. Pasricha, J. Chanale, M. K. Dongare, A.-S. Mamede, C. Lancelot and E. Payen, *Journal of Molecular Catalysis A: Chemical*, 2009, **310**, 150-158.
21. B. Wang, Y. Shen, J. Sun, F. Xu and R. Sun, *RSC Advances*, 2014, **4**, 18917.
22. H. R. Prakruthi, B. M. Chandrashekara, B. S. Jai Prakash and Y. S. Bhat, *Catal. Sci. Technol.*, 2015, **5**, 3667-3674.
23. R. W. McCabe and J. M. Adams, in *Developments in Clay Science*, eds. B. Faïza and L. Gerhard, Elsevier, 2013, vol. Volume 5, pp. 491-538.
24. F. Bergaya and G. Lagaly, in *Developments in Clay Science*, eds. B. Faïza and L. Gerhard, Elsevier, 2013, vol. Volume 5, pp. 1-19.
25. F. R. V. D. a. P. d. S. Santos, *Quim. Nova*, 2001, **24**, 345-353.
26. S. Korichi, A. Elias and A. Mefti, *Applied Clay Science*, 2009, **42**, 432-438.
27. P. Komadel and J. Madejová, in *Developments in Clay Science*, eds. B. Faïza and L. Gerhard, Elsevier, 2013, vol. Volume 5, pp. 385-409.
28. P. Anastas and N. Eghbali, *Chemical Society reviews*, 2010, **39**, 301-312.
29. G. C. Cravotto, P., *Chemical Society reviews*, 2006, **35**, 180-196.
30. C. O. Kappe, *Angewandte Chemie International Edition*, 2004, **43**, 6250-6284.
31. R. R. Pawar, S. V. Jadhav and H. C. Bajaj, *Chemical Engineering Journal*, 2014, **235**, 61-66.
32. J. P. Nguetnkam, R. Kamga, F. Villiéras, G. E. Ekodeck, A. Razafitianamaharavo and J. Yvon, *Applied Clay Science*, 2011, **52**, 122-132.

33. N. Yildiz, Z. Aktas and A. Calimli, *Particulate Science and Technology*, 2004, **22**, 21-33.
34. B. Tyagi, C. D. Chudasama and R. V. Jasra, *Spectrochimica acta. Part A, Molecular and biomolecular spectroscopy*, 2006, **64**, 273-2788.
35. J. Temuujin, T. Jadambaa, G. Burmaa, S. Erdenechimeg, J. Amarsanaa and K. J. D. MacKenzie, *Ceramics International*, 2004, **30**, 251-255.
36. S. Petit and J. Madejova, in *Developments in Clay Science*, eds. B. Faïza and L. Gerhard, Elsevier, 2013, vol. Volume 5, pp. 213-231.
37. J. B. Condon, *Surface area and porosity determinations by physisorption measurements and theory*, First edn., Elseviers B.V., 2006.
38. R. R. Pawar, H. A. Patel, G. Sethia and H. C. Bajaj, *Applied Clay Science*, 2009, **46**, 109-113.
39. R. R. Pawar, B. D. Kevadiya, H. Brahmbhatt and H. C. Bajaj, *International journal of pharmaceutics*, 2013, **446**, 145-152.
40. B. Tyagi, C. D. Chudasama and R. V. Jasra, *Applied Clay Science*, 2006, **31**, 16-28.
41. C. Ravindra Reddy, G. Nagendrappa and B. S. Jai Prakash, *Catalysis Communications*, 2007, **8**, 241-246.
42. P. Pushpaletha, S. Rugmini and M. Lalithambika, *Applied Clay Science*, 2005, **30**, 141-153.
43. M. J. da Silva, M. de Oliveira Guimaraes and A. A. Julio, *Catalysis Letters*, 2015, **145**, 769-776.
44. J. Deutsch, A. Martin and H. Lieske, *Journal of Catalysis*, 2007, **245**, 428-435.
45. Y. Gu and F. Jérôme, *Green Chemistry*, 2010, **12**, 1127.
46. F. Adam, M. Batagarawa, K. Hello and S. Al-Juaid, *Chemical Papers*, 2012, **66**.
47. M. J. Climent, A. Corma and A. Velty, *Applied Catalysis A: General*, 2004, **263**, 155-161.